

24. NEOGENE EXPLOSIVE VOLCANIC ACTIVITY OF THE WESTERN PACIFIC: SITES 292 AND 296, DSDP LEG 31

Thomas W. Donnelly, Department of Geological Sciences, State University
of New York, Binghamton, New York

INTRODUCTION

The examination of deep-sea sediments to elucidate terrestrial geological history continues to be one of the most important aspects of the Deep Sea Drilling Project. In particular, the examination of continuously cored sections near eruptive island-arc areas has proven to be the best means of determining the eruptive history of these arcs. Previous studies (Donnelly and Nalli, 1973; Donnelly, 1973) showed that the relatively primitive semiquantitative methods developed during Leg 15 could indicate the various periods of high and low-level volcanic activity in the Lesser Antilles. In relation to island-arc volcanic activity, the generation of calcalkaline magmas is generally believed to be the direct consequence of melting due to friction between a descending crustal slab beneath island arcs and the mantle above this slab. The rate of slab movement (or, at least, sea-floor spreading) is considered by many to be relatively constant, perhaps varying by a factor of two or less. Therefore, any large-scale variations in the generation of island-arc magmas with time would appear to be in contradiction to the notion of uniform spreading rates. The study of this variation with time should provide valuable insight into the question of uniformity or non-uniformity of spreading rate, or, at least, slab descent.

The western Pacific affords an excellent opportunity for further examination of the variation in volcanic activity. Sugimura and Uyeda (1973) have described the division of Japanese Neogene activity into two periods, exemplified by the classic occurrences around Hakone. Sugimura (personal communication) further modified the dates by placing a gap in activity between 13 m.y. and 2 m.y. (mid-middle Miocene through the Pliocene).

Samples from DSDP Site 296, on the Palau-Kyushu Ridge (about 500 km southeast of Kyushu Island), were examined to determine the eruptive history of this arc (Kuno, 1962). The site's location (Figure 1), makes it probable that most of the volcanic detritus is derived from southwest Japan and the Ryukyu Islands via the dominant west-to-east prevailing winds.

Kyushu-Ryukyu volcanic history may not be identical with that of east Japanese-Izu. For southwest Japan, Sugimura and Uyeda (1973) state that the northern zone had a Miocene history similar to east Japan. The median zone was active in the middle Miocene and again in the late Miocene, with activity ending in the early Pleistocene. The southern zone had important Miocene activity, at 14 m.y. and 21 m.y. The present analysis of samples from Site 296, which recorded pelagic sedimentation from the middle Miocene to Recent, partly sub-

stantiates their chronology, but suggests important modifications.

Site 292 (Figure 2) is located about 400 km southeast of the presently active volcanic center of northern Luzon and 400 km east of the center in central-southern Luzon (Neumann van Padang, 1953). The volcanic history of Luzon is not well known, thus, the record from Site 292 should provide a major contribution toward its understanding. Unfortunately, data from this site probably cannot distinguish between the northern (Cagua, Babuyan Islands) and central-southern (Mayon-Taal) volcanic centers. However, the location of Mayon nearly south of Site 292 would seem to discriminate against the southern Luzon center.

METHODS

The basic sample preparation method used involved sieving the $>43\mu$ fraction from 2 cc of sediment, acidifying in 0.1N HCl to remove calcareous fossils, and weighing the residue. The fraction of volcanic debris was estimated from slides studied under the microscope.

The accumulation rate of total volcanic material, and of plagioclase crystals, separately, is calculated using the estimated total sedimentation rates for the sediment. For this study, the shipboard paleontology was used, with the depth-time curves for Sites 292 and 296 being shown in Figures 3 and 4.

The validity of the method for estimating explosive activity, and, from this, igneous activity in general, depends on several assumptions. These are: (1) that the sample is representative of a wide time interval; (2) that the debris deposited is directly related to magma production; (3) that the debris surviving diagenesis is representative of that originally deposited; and (4) that the debris coarser than 43μ is representative of the original material produced. Some of these assumptions are difficult to defend a priori; however, the relative smoothness of the trends in activity with time and the crude correlation from area to area tend to support the method.

Problems Inherent in the Estimations

Diagenetic alteration may alter or eliminate some of the originally deposited volcanic materials, especially glass. For example, because of the relatively slow accumulation rates at Site 292, from about 35 to 110 meters (Figure 3), most of the glass was converted to phillipsite. The alteration of glass in the older, more rapidly accumulated, volcanic sediment (about 110 to 140 m), apparently resulted from a long exposure to seawater during an early Miocene hiatus (at about 110

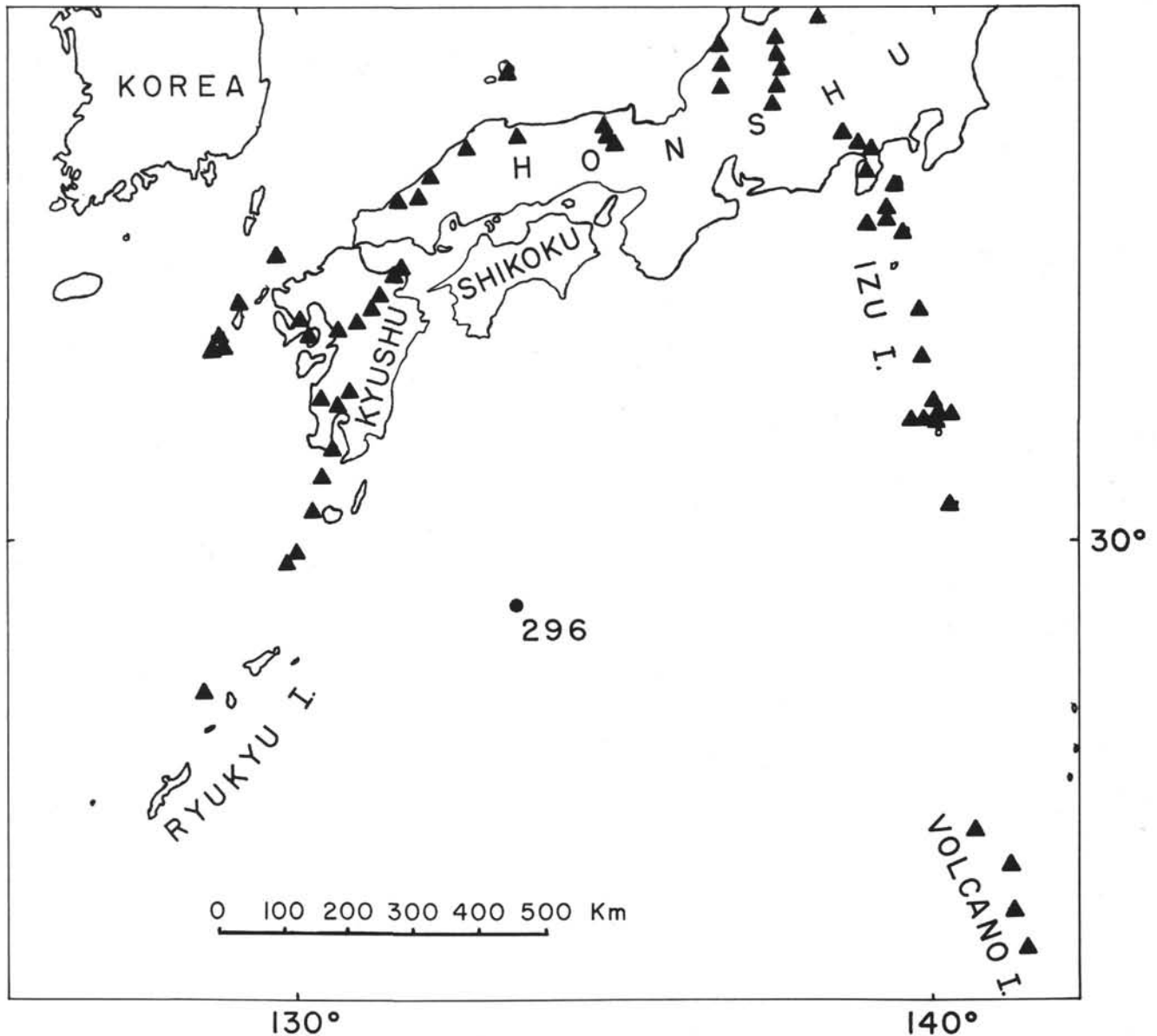


Figure 1. Location map showing for Site 296 Quaternary volcanic centers for Japan and adjacent areas (Kuno, 1962).

m). The absence of glass correlates well with the appearance of the phillipsite.

Thus an alternative method might be to estimate authigenic minerals instead of glass. However, the fine-grained nature of the phillipsite, and the uncertainty on the authigenic origin of minerals, present difficulties which question the validity of this alternative estimation. Because of this, the principal determination is placed on the amount of plagioclase feldspar which, although sometimes corroded (Donnelly, 1973), is the most resistant abundant constituent of volcanic debris.

Questions are also raised as to whether the amount of plagioclase is reasonably constant in volcanic debris during periods of high and low eruptive activity. Evidence from Site 296 (Table 1) shows that glass is relatively more abundant during periods of high eruptive ac-

tivity. Thus, estimates of variations in volcanic activity based on plagioclase alone might be underestimated.

Even when glass is fairly well preserved, not all volcanic debris is recognizable. The porphyritic andesitic glass from Sites 292 and 296 is commonly altered and nearly indistinguishable from fine-grained authigenic mineral aggregates.

Plagioclase, quartz, and K-feldspar of volcanic origin are not always easily distinguished from terrigenous debris deposited by turbidity currents. For example, quartz is found associated with epidote at Site 292, thus implying that the sediments might be sedimentary detritus with a low-grade metamorphic provenance.

The problem of K-feldspar is more complex. Authigenic K-feldspar, which is abundant in the Caribbean (Donnelly and Nalli, 1973), is even more abundant

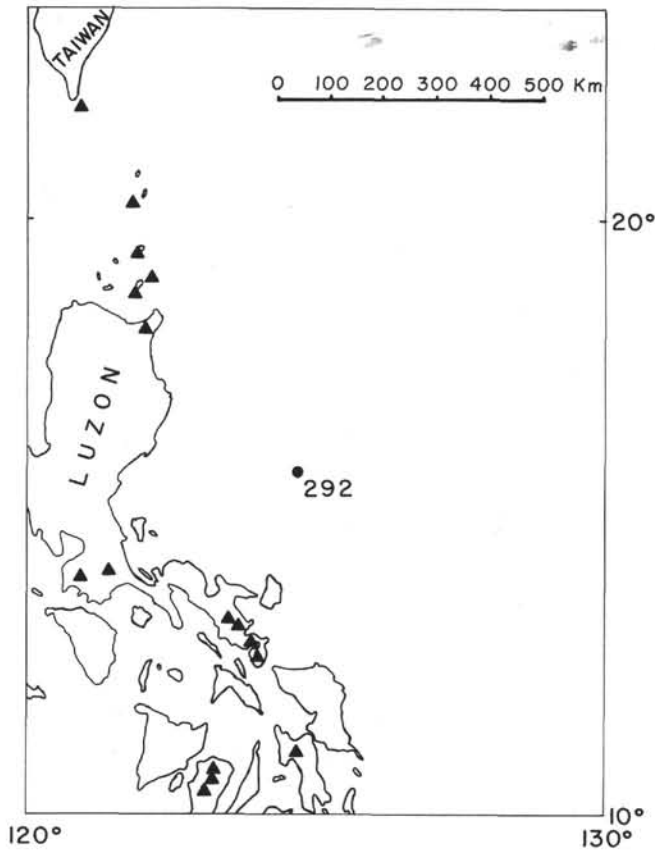


Figure 2. Location map showing Site 292 and Recent volcanic centers for the northern Philippines and adjacent areas (Neumann van Padang, 1956).

in the sediments of Sites 292 and 296. However, the grains are less euhedral than in the Caribbean occurrences and the distinction from volcanic K-feldspar is difficult. However, the results are not strongly affected by a misallocation of the feldspar types.

Constituents and Calculations

Microscopically, the following constituents are distinguished: clear, porphyritic, and brown glass; plagioclase; K-feldspar (volcanic versus authigenic distinguished); quartz; red, green, or brown hornblende; orthopyroxene; clinopyroxene; biotite; zircon; and apatite. The percentage of total volcanic material, clear glass, plagioclase, and "mafics" are found in Table 1 and illustrated on Plates 1-4. These constituents and some additional ones seen in samples from Sites 293, 294, and 295 are tabulated in Table 2.

Figures 5 and 6 show the logarithm of the rate of accumulation of total volcanic material, and of plagioclase alone, plotted against age. The rate of accumulation is calculated as follows: rate of accumulation ($\text{g}/\text{cm}^2 \text{ m.y.}$) = wt of residue from 2 cc of sediment (g) \times total sedimentation rate (m./m.y.) \times 50 \times fraction total volcanic material (or plagioclase).

It should be stressed that, although the method is rapid, the results are largely based on estimates of constituent abundance.

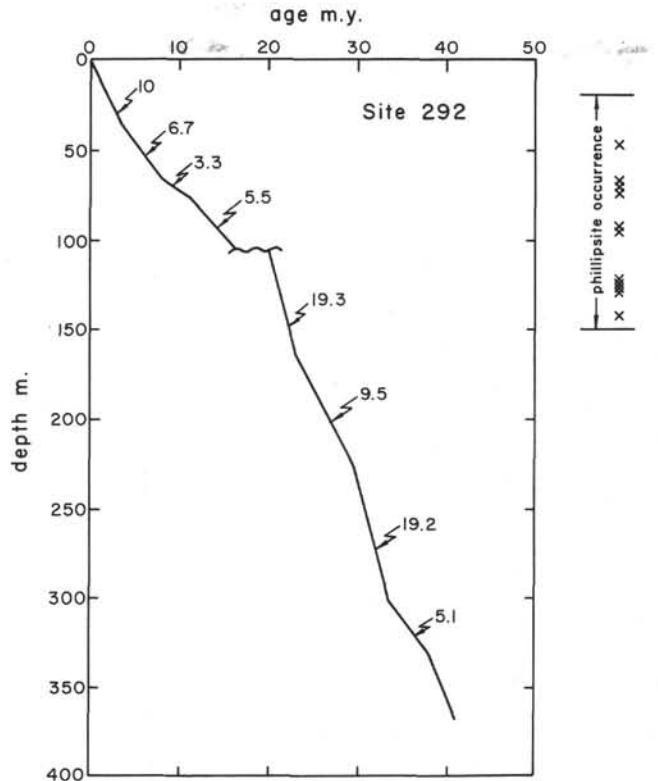


Figure 3. Age-depth curve for Site 292, showing total sediment accumulation rates used for construction of Figure 7.

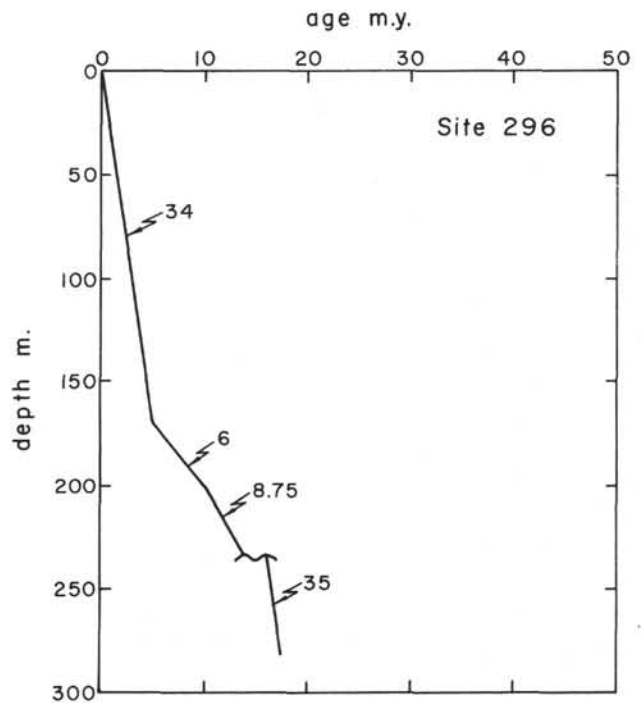


Figure 4. Age-depth curve for Site 296, showing total sediment accumulation rates used for construction of Figure 8.

TABLE 1
Constituents Distinguished From Samples at Sites 292 and 296

Sample (Top of Interval in cm)	Age	Wt Res	Volc (%)	Glass (%)	Plag (%)	Maf (%)	Hb	Orpx	Clpx	Other
Site 292										
1-1, 74	0.09	0.025	60	30	29	10	45	14	42	Q, Bi, red Hb
1-2, 90	0.29	0.331	90	45	18	2	(0)	(0)	(100)	
1-3, 85	0.47	0.184	95	65	23	5	92	8	0	red Hb
1-4, 7	0.55	0.03	95	50	35	16	100	tr	tr	red Hb
2-1, 143	0.96	0.05	80	5	68	17	100	tr	tr	Bi, red Hb, KF
2-2, 66	1.05	0.017	20	5	90	5	48	21	30	KF, red Hb, AKF
2-3, 91	1.26	0.1055	90	70	20	5	16	16	68	KF
3-1, 148	2.12	0.08	40	80	15	5	7	0	93	Bi, Ep
3-2, 15A	2.14	0.6255	95	65	14	1	25	0	75	Bi, Ep
3-2, 112	2.26	0.018	30	tr	40	4	31	0	69	Bi, Q, AKF*, P, Ep
3-3, 17	2.32	0.016	80	tr	85	15	72	2	27	Bi, Ep, P, Z
3-4, 30	2.52	0.003	90	0	87	13	71	0	29	Q, Ep, AKF, P
4-1, 91	3.20	0.003	85	tr	90	10	93	1	6	red Hb*, Ep, P
4-2, 65	3.35	0.005	70	1	81	10	94	0	6	Bi, red Hb, Q, Ep, P
4-3, 62	3.53	0.002	30	1	96	2	76	0	24	Bi, red Hb, Ep, P, AKF
4-4, 127	3.79	0.003	90	tr	83	12	83	0	17	Ep
4-5, 103	3.94	0.002	20	0	70	20	64	0	36	Bi, red Hb, KF*, P
5-1, 22	4.27	0.0012	40	1	94	2	69	2	29	red Hb, Q, Ep*, AKF*
5-2, 74	4.51	0.001	30	0	80	20	65	0	35	Bi, red Hb, Ep, AKF, Z, P
5-3, 63	4.68	0.0015	20	0	83	20	41	0	59	Ep, AKF
5-4, 45	4.84	0.0012	70	3	87	5	88	0	12	Ep, AKF, Z
5-5, 24	5.00	0.0015	50	0	89	5	76	0	24	Q, Zr, Ep, AKF
5-6, 60	5.22	tr	40	1	89	10	89	0	11	Bi, red Hb, AKF, P
6-1, 128	5.55	tr	10	2	83	15	74	0	26	red Hb, Ep, AKF, P
6-2, 35	5.62	0.008	95	3	92	5	91	0	9	P*
6-3, 68	5.84	0.0012	10	tr	89	11	100	0	tr	red Hb, Bi, Ep, AKF
6-4, 115	6.08	0.001	80	5	94	5	100	0	0	Q, KF, Bi
6-5, 86	6.23	0.0005	25	0	80	15	85	0	15	KF, Bi, red Hb, Ap, Ep, AKF, P, Z
6-6, 134	6.47	0.0004	30	2	83	15	100	0	tr	KF, (Z)
7-1, 53	6.61	0.0005	40	tr	90	10	100	tr	tr	Q, Ep, AKF, Z
7-2, 141	7.11	tr	50	5	90	5	85	0	15	Bi, Ep, AKF, P
7-3, 41	7.22	0.0015	30	0	80	20	100	0	tr	P*
7-4, 59	7.57	tr	30	5	90	3	(63)	(0)	(37)	Q, Z, AKF, P
7-5, 20	7.81	0.0005	90	0	85	15	67	0	33	Bi, Ep, Z, AKF
7-6, 91A	8.28	0.2	60	0	60	40	30	0	70	Bi*, KF, Ap, P
7-6, 127	8.35	0.002	80	0	75	25	100	0	tr	red Hb, P
8-1, 127	8.77	tr	50	2	89	9	73	0	27	red Hb, Zr, Ep, AKF, P
8-2, 48	9.29	tr	50	5	84	10	90	0	10	Bi, Ep, P*, AKF
8-3, 77	9.30	0.0025	90	0	83	17	77	0	23	Bi*, AKF, P*
8-4, 69	9.60	tr	40	0	85	5	88	0	12	Q*, red Hb, Bi, Ep, P
8-5, 23	9.82	0.001	50	10	75	15	95	0	5	Bi, red Hb, Ep, Z, AKF, P
8-6, 52	10.20	tr	30	2	95	3	(67)	(0)	(33)	Q, KF, Bi, Ep, P
9-1, 136	10.80	tr	30	0	100	tr	(tr)	(0)	(0)	Q, P*
9-2, 109	11.06	tr	40	1	94	5	(70)	(0)	(30)	Bi, Q, P
9-3, 22	11.16	0.0012	60	1	68	30	100	tr	tr	KF, red Hb, Bi, Ap, AKF, P
9-4, 60	11.47	tr	10	2	93	5	(100)	(0)	(0)	Q, P
9-5, 90	11.76	0.0005	70	2	83	11	90	0	10	KF, Ep, Z, P, AKF
10-1, 105	12.35	0.001	10	1	64	5	(80)	(0)	(20)	Bi*, KF*, AKF, P
10-2, 113	12.61	0.0003	40	5	70	9	(66)	(22)	(12)	red Hb, KF, Bi*, P
11-2, 129	14.18	0.001	10	2	86	10	90	0	10	red Hb, Ep, Z, P*
11-4, 39	14.52	0.015	50	tr	96	4	42	0	58	Q, Ep, P*, Z
11-6, 60	15.04	tr	20	5	50	5	(80)	(0)	(20)	Bi*, AKF, P
12-2, 48	20.39	0.002	50	0	80	20	81	0	19	Bi*, KF, red Hb, AKF*, Z
12-3, 114	20.49	tr	30	tr	90	5	(100)	(0)	(0)	KF, Z, AKF
12-5, 72	20.61	tr	60	5	85	10	100	0	0	red Hb, Ep, AKF, Z, P
13-2, 34	20.82	tr	70	0	95	tr	21	0	79	?Garnet, Z
13-3, 33	20.89	tr	40	0	95	5	(100)	(0)	(0)	Bi, red Hb, AKF*, KF
13-5, 141	21.08	tr	10	10	70	10	100	0	tr	KF, Z
14-1, 119	21.23	0.0003	75	2	88	8	(75)	(25)	(0)	Bi*, P*, KF
14-3, 23	21.33	0.0012	80	tr	90	5	100	0	0	Bi*, red Hb*, AKF, P
14-4, 71	21.42	0.001	60	5	85	10	100	0	tr	Bi, red Hb, Z, P
14-6, 66	21.55	tr	50	tr	95	5	(67)	(0)	(33)	Bi, P
15-1, 135	21.68	0.001	80	tr	93	7	79	0	21	Ep, P, Z
15-3, 60	21.78	tr	70	tr	95	5	92	0	8	Bi, Ep, P
15-5, 146	21.96	0.0005	50	tr	95	5	92	0	8	red Hb, Z
15-6, 7	21.96	tr	65	2	85	3	(90)	(0)	(10)	P, AKF*

TABLE 1 - Continued

Sample (Top of Interval in cm)	Age	Wt Res	Volc (%)	Glass (%)	Plag (%)	Maf (%)	Hb	Orpx	Clpx	Other
16-2, 49	22.15	0.02	60	5	78	12	93	0	7	red Hb*, KF*, Bi*, Ep, P
16-4, 55	22.29	0.017	50	30	65	5	42	31	27	red Hb, Bi, KF, Z
16-5, 80	22.37	tr	50	10	80	10	97	0	3	red Hb, Bi, KF, Ep, Z
17-1, 133	22.55	0.06	75	80	15	5	7	0	93	Bi*
17-2, 104	22.61	0.108	90	70	25	5	(12)	(0)	(88)	Bi*
17-4, 144	22.77	0.05	75	40	40	20	64	0	36	Bi*, red Hb
17-5, 46	22.79	0.065	10	8	80	9	81	4	15	Bi*, red Hb
18-1, 143	23.00	0.045	30	70	14	16	40	9	51	Bi*, red Hb
18-5, 89	23.54	0.02	30	10	65	15	26	0	74	Bi*, KF
19-2, 37A	23.99	0.193	85	0	25	5	0	79	21	
19-4, 15	24.27	0.075	95	70	22	8	43	6	51	
19-6, 78	24.63	0.01	20	49	41	2	12	0	88	red Hb
20-2, 105	25.01	0.017	50	50	10	tr	13	19	68	
21-2, 73	25.92	0.0055	40	65	38	tr	(33)	(17)	(50)	
21-4, 116	26.27	0.064	80	96	4	tr	(0)	(0)	(100)	
22-2, 57	26.86	0.162	95	85	10	5	100	0	0	red Hb
22-3, 115	27.07	0.085	70	0	4	1	0	19	81	Bas. Glass
23-3, 14	27.91	0.04	2	0	0	0	0	0	0	Bas. Glass
24-3, 96	28.95	0.0855	50	0	0	0	0	0	0	Bas. Glass
25-2, 109	29.64	0.0185	2	10	20	0	0	0	0	Bas. Glass
26-2, 94	30.13	(0.022)	2	0	80	20	(0)	(0)	(100)	
27-1, 92	30.55	L	tr	tr	0	0	0	0	0	
29-1, 88	31.55	L	tr	0	tr	0	0	0	0	
31-2, 70	32.62	0.0139	tr	0	tr	0	0	0	0	
33-1, 0	33.50	(0.08)	0	0	0	0	0	0	0	
34-2, 2	35.57	0.0097	5	40	60	0	0	0	0	KF, Q
35-3, 9	37.64	L	5	0	100	0	0	0	0	KF
36-1, 18	38.35	L	(90)	(smear slide only)						Riebeckite, authigenic Glaucophane, KF, Clpx, Plag, Glass
36-3, 17	38.58	L	5	tr	100	0	0	0	0	KF
37-3, 116	39.36	L	10	85	5	0	0	0	0	
38-1, 73	39.82	L	40	0	9	1	0	0	tr	Bas. Glass
39-1, 98	40.55	L	20	0	100	tr	tr	0	tr	
Site 296										
1-1, 94	0.03	0.015	65	70	15	10	30	50	20	
1-3, 77	0.11	0.012	95	50	28	2	27	42	31	
2-2, 131	0.27	0.062	95	75	20	5	2	55	43	KF, Bi
2-3, 20	0.29	0.05	95	94	5	tr	33	50	17	
2-3, 120A	0.31	0.012	70	10	63	2	6	56	39	
2-6, 65	0.43	0.291	95	90	9	1	tr	0	100	
3-2, 131	0.55	0.6675	95	85	10	5	55	32	13	Bi*, red Hb, P
3-4, 110	0.64	0.07	85	15	10	tr	0	tr	0	
4-1, 124	0.83	0.03	95	60	30	5	9	41	50	
4-3, 20	0.89	0.006	70	20	58	2	10	40	50	AKF
5-1, 115	1.06	0.005	60	70	25	2	18	39	43	Bi
5-4, 11	1.16	0.07	60	70	20	5	(0)	(tr)	(100)	Bi
6-2, 12	1.36	0.116	75	40	45	5	0	80	20	KF
6-5, 63	1.50	0.0005	40	15	80	tr	(0)	(20)	(80)	Bi, Q*, Z, AKF
7-3, 143	1.72	0.005	60	5	88	5	0	78	22	
7-4, 92	1.75	0.0214	90	30	40	10	0	70	30	
8-1, 101	1.90	0.02	50	60	30	5	0	80	20	
8-3, 61	1.97	0.08	95	85	14	1	25	41	34	Ap, KF
8-3, 123A	1.99	0.07	65	10	29	1	6	38	56	Z
9-2, 57	2.21	0.02	60	50	30	10	15	38	47	AKF
9-5, 21	2.33	0.025	50	50	40	10	88	0	12	red Hb
10-2, 102	2.50	0.003	85	20	55	12	39	30	30	
10-4, 132	2.60	0.04	10	65	35	tr	(0)	(tr)	(0)	
10-6, 146	2.69	0.0435	95	78	15	tr	69	27	3	red Hb
11-1, 145	2.75	0.006	95	25	71	4	47	41	11	Bi
11-4, 33	2.85	0.01	90	60	35	3	48	30	22	AKF, Z
12-1, 98	3.01	0.02	95	94	5	1	0	55	45	Z
12-5, 126	3.20	0.008	90	25	50	10	60	20	20	KF
13-1, 95	3.29	0.012	65	45	35	15	0	100	0	
13-3, 132	3.39	0.017	90	50	46	1	26	56	18	Q, AKF
14-2, 138	3.64	0.065	95	95	4	tr	(100)	(0)	(0)	
14-3, 51	3.66	0.02	95	38	30	10	44	36	20	red Hb, KF
14-6, 87	3.81	0.02	30	5	70	25	32	48	20	

TABLE 1 - Continued

Sample (Top of Interval in cm)	Age	Wt Res	Volc (%)	Glass (%)	Plag (%)	Maf (%)	Hb	Orpx	Clpx	Other
15-2, 103	3.90	0.085	95	90	8	1	20	60	20	Zr, Z
15-3, 32A	3.92	0.765	100	90	7	0	0	0	0	
15-3, 79	3.94	0.255	95	95	5	0	0	0	0	
16-1, 122	4.14	0.017	95	60	28	4	20	53	27	red Hb
16-4, 124	4.27	0.008	40	35	50	15	23	35	41	KF
16-6, 52	4.34	0.10	95	1	22	2	0	66	34	Q, AKF, Z
17-3, 136	4.51	0.009	95	4	92	2	44	44	12	Z
17-5, 71	4.58	0.02	50	20	70	10	40	40	20	
18-1, 58	4.68	0.001	80	tr	95	4	50	50	tr	red Hb
18-2, 98	4.73	0.007	50	1	96	3	80	0	20	
19-2, 60	5.02	0.042	75	40	50	10	64	24	12	Bi*
19-4, 94	5.65	0.025	95	68	20	10	61	24	15	Bi*
20-1, 146	6.50	0.001	50	0	75	24	100	0	0	red Hb, KF
20-2, 75	6.63	0.0002	40	tr	99	1	(100)	(0)	(0)	Z, AKF
20-3, 105	6.93	0.0005	50	15	80	3	(67)	(0)	(33)	red Hb
20-4, 95	7.17	tr	15	5	95	tr	(70)	(0)	(30)	Bi, AKF
21-1, 100	8.00	(0.01)	1	30	70	0	0	0	0	
21-2, 46	8.17	0.002	60	1	95	4	91	9	0	red Hb, Bi, AKF
21-3, 92	8.48	0.055	95	70	18	2	6	39	56	
21-4, 102	8.67	0.045	95	94	2	1	(14)	(29)	(57)	
21-5, 133	9.05	0.017	90	10	70	tr	(0)	(57)	(43)	
21-6, 94	9.23	0.02	90	40	19	1	22	28	50	red Hb, Z
22-1, 141	9.65	0.002	75	0	49	1	(70)	(0)	(30)	red Hb*, Z
22-2, 38	9.73	0.005	15	40	40	20	60	0	40	Bi
22-3, 17	9.95	0.001	40	75	24	1	(0)	(0)	(100)	Bi, AKF
22-4, 9	10.10	0.0035	50	75	24	tr	(0)	(30)	(70)	
22-5, 138	10.44	0.0002	20	1	95	4	(100)	(0)	(0)	red Hb
22-6, 29	10.49	tr	75	5	90	5	50	7	43	Bi
23-1, 133	10.83	0.027	5	80	20	0	0	0	0	
23-2, 118	10.99	(0.03)	50	80	17	1	(0)	(20)	(80)	
23-3, 69	11.11	0.0025	90	75	23	2	100	tr	0	Bi, red Hb
24-1, 41	11.82	0.0015	90	70	20	6	50	33	17	Bi
24-2, 110	12.07	0.012	70	80	17	3	36	36	28	Q, Bi, AKF
24-3, 91	12.22	0.002	40	40	48	11	30	30	40	
24-4, 32	12.40	0.002	50	30	65	4	55	14	31	
24-6, 130	12.78	0.003	80	60	25	5	81	2	17	
25-1, 89	12.96	0.015	80	75	20	5	100	tr	0	Bi, KF
25-2, 102	13.14	0.017	95	65	20	8	42	25	33	KF
25-3, 114	13.33	0.04	90	45	40	10	46	27	27	
25-4, 111	13.50	0.031	85	78	15	5	0	80	20	
26-1, 130	16.02	0.03	60	68	25	5	28	21	51	
26-2, 67	16.04	0.051	50	50	40	10	30	50	20	
26-4, 141	16.15	0.017	60	15	80	5	22	46	32	Ap
27-2, 124	16.32	0.018	80	10	85	4	4	50	46	Bi, Z, AKF
27-3, 85	16.35	0.047	80	5	20	5	5	24	71	Z
28-2, 84	16.56	0.175	90	90	9	tr	(0)	(33)	(67)	Z
28-3, 42A	16.59	0.872	100	98	1	tr	(0)	(tr)	(tr)	
28-3, 96	16.61	0.301	40	96	4	tr	(0)	(100)	(0)	KF
28-4, 120A	16.65	0.1625	98	95	5	tr	(tr)	(0)	(tr)	Bi*, Zr
28-4, 22	16.63	L	30	60	40	tr	(0)	(tr)	(0)	
28-5, 98	16.69	0.06	85	90	8	tr	55	27	18	
29-1, 13	16.76	0.06	85	90	8	1	29	29	42	Bi
29-3, 20	16.84	0.316	95	95	9	tr	(0)	(tr)	(tr)	
29-5, 36	16.92	0.03	40	40	28	1	0	9	91	

Note: A = labeled volcanic ash; Age = estimated age in m.y., taken from recorded depth and depth vs. age curves by linear interpolation; Wt. Res = weight in g of residue (325 mesh = 43 μ) from 2-cc sample; L = lithified, parentheses for poorly estimated weight due to lithification; % Volc = percent of volcanic material in aliquot of total residue; tr = trace amount; % Glass = percent of clear glass in total volcanic material of aliquot; % Plag = percent of plagioclase in total volcanic material of aliquot; % Maf = percent of mafic minerals in total volcanic material of aliquot; Hb, Orpx, and Clpx = percent of brown or green hornblende, orthopyroxene, and clinopyroxene, respectively, in total of these three minerals, parentheses indicate less than 10 grains counted total; Other: Q = quartz (volcanic or terrigenous), KF = K feldspar, (generally volcanic or terrigenous, but perhaps including some authigenic); AKF = authigenic K-feldspar; Bi = biotite; red Hb = red hornblende; Ap = apatite; Zr = zircon; Ep = epidote; Z = zeolite (indet.); P = phillipsite; Bas. Glass = clear basaltic glass (brown, low positive relief). Asterisks indicate an exceptional amount.

TABLE 2
Constituents Distinguished From Samples at Sites 293, 294, and 295

Sample (Top of Interval in cm)	(%) Volc	(%) Glass	(%) Plag	Hb	Orpx	Clpx	Other
Site 293							
2-2, 140	80	0	70	50	0	50	KF
2-5, 27	50	6	90	100	0	tr	
2-5, 47	70	1	60	(70)	(30)	tr	
2-5, 59	80	3	70	67	tr	33	red Hb, Bi, KF, Z
2-5, 64	95	0	83	0	80	20	
4-2, 81	95	tr	65	67	tr	33	Ap, red Hb
5-4, 133	40	0	100	tr	0	0	Wood, KF
6-2, 25.5	60	tr	95	38	13	63	red Hb
6-2, 100	50	?	50	0	0	(100)	
8-2, 77	80	0	100	25	75	tr	
10-2, 69	30	0	30	0	0	0	
15-1, 95	95	0	94	95	0	5	Bi, KF, red Hb
15-1, 101	40	0	50	10	0	90	Z, AKF
15-1, 130	40	0	80	tr	0	tr	FD
16-3, 79	70	0	20	58	8	34	KF, red Hb, FD
17-3, 81	50	0	60	0	0	0	Ap*, Bi
18-1, 62	tr	0	tr	tr	0	0	FD
Site 294							
1-4, 70	85	0	70	50	0	50	
3-5, 87	tr	0	tr	0	0	0	unident. opaque
4-3, 78	5	0	100	tr	0	0	FD, auth Q?
4-4, 146	5	0	100	tr	0	0	Ap, FD, MN
6-1, 62	0	0	0	0	0	0	MN, FD
Site 295							
1-5, 73	50	0	80	0	0	tr	Q*, FD, AKF
2-2, 42	60	0	60	0	0	0	Mt, FD
2-6, 106	20	0	100	0	0	0	FD
3-4, 35	2	0	100	0	0	0	Q, FD

Note: Same as for Table 1, except that Wt Res, %MAF, and Age are omitted. These samples have not been treated with acid and represent a coarser fraction (62μ rather than 43μ) than those reported in Table 1. One sample (293-15-1, 130 cm) has abundant carbonate-coated grains of volcanic crystals, comparable grains would not have been seen in the Site 292 and 296 samples. Additional symbols: FD = fish debris; Mt = magnetite; MN = micronodules.

PETROGRAPHY

The volcanic debris from Sites 292 and 296 is fairly homogeneous in character. It generally consists of well-sorted, highly angular, fine debris, suggesting dispersal as wind-borne rather than as pumice-rafted debris. Glass is generally dominant in fresher samples, with plagioclase most abundant in altered samples. Variations in the relative amounts of clear glass, plagioclase, and mafic minerals are apparently independent of later alteration. Some variation evidently results from a relatively high proportion of glass in the samples with the highest proportion of total volcanics. Still other variations are not explained, such as the occasional high-mafic content. High-biotite and other mineralogically peculiar samples evidently reflect variations in magmatic chemistry.

Coarser crystalline constituents, especially plagioclase and clinopyroxene, are characteristically shattered with conchoidal fractures, evidently reflecting highly explosive eruptive activity. Hornblende is generally cleaved, and the smaller grains tend to be euhedral, or subhedral as a result of magmatic resorption. A preserved glass investment on many of these small grains (pyroxenes,

hornblende, quartz) shows that this rounding does not result from diagenesis.

Clear Glass

Clear glass is generally the dominant form of glass. It is rarely entirely absent, even when authigenic minerals are abundant. The glass exists as bubble, or tubular pumice. Some of the bubble glass evidently had relatively large diameter vesicles; relics consist of nearly flat, angular plates. Altered glass is commonly more equant than fresh glass, and angular, almost polyhedral blocks are common. Bubble glass is commonly more abundant than tubular pumice.

Porphyritic Glass

Porphyritic, andesitic glass is generally subordinate, but widely occurring. It varies towards the clear form, less commonly, to the brown form. It is generally highly altered, and some was probably misidentified as non-volcanic authigenic mineral aggregates. In doubtful cases, the presence of plagioclase microlites facilitates identification. Aside from plagioclase, one sample (296-16-6, 52 cm) contains orthopyroxene microphenocrysts.

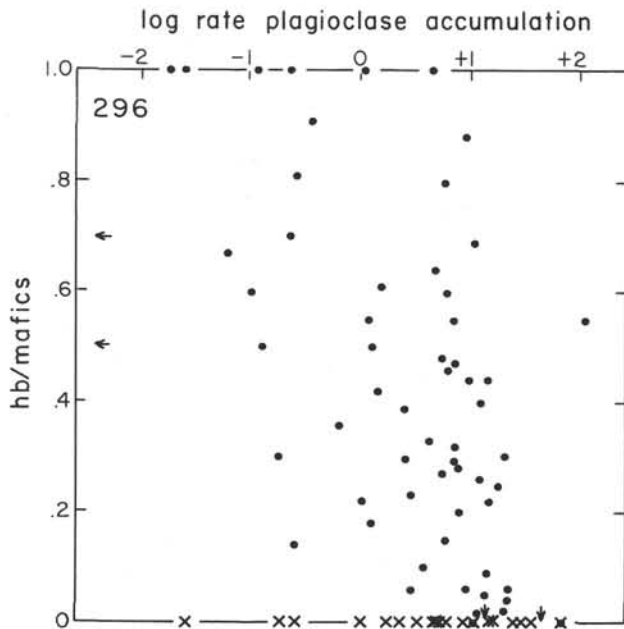


Figure 5. Curve showing for Site 296 the relationship between the proportion of brown and green hornblende to total mafics (sum hornblende + clinopyroxene + orthopyroxene) against the log of accumulation rate of volcanic plagioclase ($\text{g}/\text{cm}^2 \text{ m.y.}$). Arrows indicate trace amounts of sediments; "x" symbols the absence of hornblende.

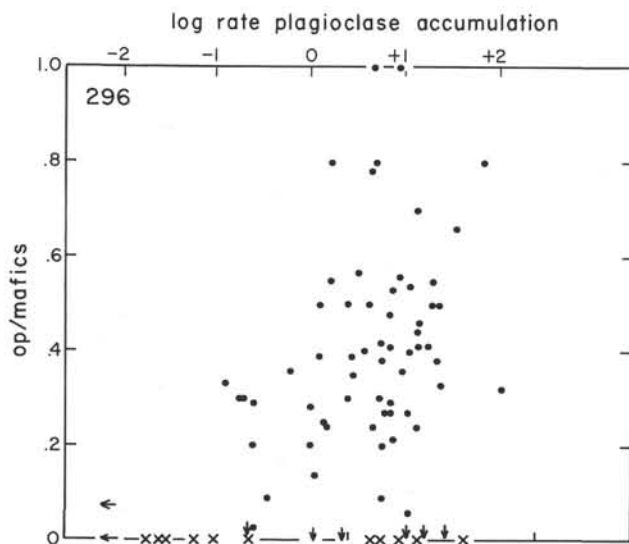


Figure 6. Curve showing for Site 296 the relationship between the proportion of orthopyroxene to total mafics (as in Figure 5) against the log of accumulation rate of volcanic plagioclase ($\text{g}/\text{cm}^2 \text{ m.y.}$).

At Site 292, porphyritic glass is scarce in the upper part (Cores 1 to 8) with only one sample in Core 3 having large amounts. In the lower part (Cores 19 to 22), this glass is more conspicuous. At Site 296, it is far more common than at Site 292 being the predominant volcanic constituent in Cores 3, 8, 16, and 22.

Brown Glass

Fresh brown glass has a refractive index similar to Caedex and is probably basaltic. It is generally non-porphyritic, or contains unrecognizably small micro-lites. It is of bubble form, evidently representing scoria. This glass is in most cases scarce, but conspicuous at Site 292 in Cores 1, 3, 10 (where it is palagonitized in 292-10-1, 105 cm), Cores 23-25, and in Core 27 from Site 296.

Plagioclase

Plagioclase is the most ubiquitous of the volcanic mineral species. Although generally anhedral (conchoidally or otherwise fractured irregularly), a few grains are euhedral. Most grains are compositionally zoned, and show simple twinning. Polysynthetic twinning is relatively rare, and these grains (Site 292) may be sedimentary detritus. The plagioclase has a variable, but commonly low refractive index. Possibly, much of the plagioclase has reacted with pore waters to generate more sodic rim.

The recognition of plagioclase, many grains of which are untwinned, requires some experience. It is based on the visible compositional zoning, and a distinctive dispersion which gives characteristic brown and purple extinction colors. Much plagioclase also contains two-phase fluid or glass inclusions.

K-feldspar: Volcanic and Authigenic

K-feldspar is generally a scarce constituent. Although it was more conspicuous at Site 292, there was no particular pattern of occurrence of this mineral at either site.

Volcanic K-feldspar is water clear, commonly simply twinned, showing some optical zoning and dispersion. The very low refractive index and low negative 2V are also distinctive.

Authigenic K-feldspar is rarely as euhedral as had been found in Caribbean sediments (Donnelly and Nalli, 1973). Some grains are commonly crowded with inclusions, often arranged more or less parallel to the C-axis. Some authigenic K-feldspar occurs as formless, multicrystalline aggregates, recognized by their birefringence, relief, and texture. Authigenic K-feldspar occurs in samples from Sites 292 and 296, but it is especially common in that part of Site 292 where glass is virtually absent.

Quartz

Quartz grains of purely volcanic origin are scarce. All of the four occurrences from Site 296 are presumed to be volcanic, as well as the occurrence in Core 1 from Site 292 where quartz grains are invested with glass. The scattered quartz occurrences below Core 2 at Site 292 are considered to represent sedimentary dispersal rather

than a volcanic origin. These occurrences are suspiciously parallel with occurrences of epidote and polysynthetically twinned plagioclase, all of which are considered to originate in a low-grade metamorphic environment. In samples of Core 292-13 a lone grain of pink garnet was also found. Characteristic tiny fluid inclusions (which are all of one phase) are present in the presumably metamorphic quartz.

Zeolites: Phillipsite

The only zeolite positively identified (optically or by X-ray diffraction) was phillipsite. At Site 292 the appearance of phillipsite correlates with the disappearance of glass, providing strong circumstantial evidence for a volcanic origin. At Site 296, phillipsite was only positively identified in one sample, but several other occurrences of "zeolite" at the same site are probably phillipsite.

Most of the phillipsite is in the form of characteristic angularly terminated prisms. In grain residues, however, most zeolite occurs in odd multicrystalline lumps showing numerous small crystalline faces and reentrants.

Epidote

This mineral occurs in Cores 3 through 16 from Site 292. It is rarely common, but easily recognized. Most grains are of one crystal only, but a few are multicrystalline. Epidote is presumed here to be an indicator of transport by turbidity current from a metamorphic source. The limited abundance of epidote (and co-occurring presumably metamorphic quartz) indicates that most of the crystalline debris at this site represents volcanic activity.

Hornblende

Hornblende is the second most widespread mineral species in these sediments. There is no positive evidence for metamorphic amphibole (with the epidote-quartz suite at Site 292). Most hornblende occurs in euhedral (cleaved?) or subhedral rounded grains. The commonest colors are shades of brown to olive to green, but bright red hornblende also occurs throughout in small quantities.

Some distinctively colored varieties probably merit further work: very pale-colored (292-11-6, 60; 296-21-2, 46; and 296-24-4, 32); conspicuous golden varieties (292-13, 296-5, 296-20; and 296-24); hornblendes with a high optical absorption, possibly representing a more alkalic magmatic origin, (292-16-2, 49 and 292-16-5, 80); a deep brown hornblende (292-18-1, 143); and a hornblende, pleochroic in pink and green, (296-24-2, 110; 296-22-1, 141; 296-23-3, 69; and 292-6-2, 35).

A most distinctive euhedral deep-green riebeckite (length fast, n_x about 1.69) was seen in an alkalic ash from Site 292 (292-36-1, 18), occurring with a euhedral clinopyroxene, glass, K-feldspar, plagioclase, and authigenic glaucophane.

Glaucophane

The most unusual mineral species found was glaucophane, which occurred as tiny prisms in Sample

292-36-1, 18. The euhedral crystal form, and occasional intergrowth with evidently authigenic K-feldspar implies that it is an authigenic product of the alteration of an especially alkalic ash which produced augite, riebeckite, and K-feldspar. The glaucophane is deeply colored, distinctively pleochroic, but evidently concentrically zoned on a fine scale. The slow refractive index of about 1.63, implies a low iron content. However, these grains are length fast, characteristic of crossite.

The designation of an authigenic nature for glaucophane is based on its occurrence as rather long, thin prisms, some of which are aggregated in a radial pattern, and occasional intergrowth with authigenic (?) feldspar. Another heretofore low-grade metamorphic mineral, spessartine, was found as an evident authigenic mineral in Leg 15 sediments (Donnelly and Nalli, 1973).

Biotite

Biotite is minor but widespread, especially at Site 292. It is invariably brown, and occasionally shows a hexagonal subhedral crystal form. It often has polygonal holes; the hexagonal ones were probably occupied by apatite, but other holes appear to have been occupied by a monoclinic mineral.

The biotite of Site 292 shows a pattern of alteration parallel to, but not identical to, that of glass, and the appearance of phillipsite. Cores 1 and 2 have altered biotite, Cores 3 through 10 have mainly altered biotite, with fresh grains in Cores 3, 4, 7, 8, and 10. Cores 14 through 18 have only fresh material.

Apatite

Apatite is far less common in the western Pacific than it had been in older volcanic material from the Caribbean (Donnelly, 1973). The occurrences are noted in Tables 1 and 2.

Clinopyroxene

In all probability all of the clinopyroxene found at both sites is augite. It is invariably pale green, rarely with a distinct yellowish tinge. Particularly pale grains were found in 296-16, and especially deeply colored green grains were seen in Cores 1, 3, 17, and 18 of Site 292 and Cores 21 and 22 from Site 296.

Orthopyroxene

Orthopyroxene (all of which is probably hypersthene) is less common than clinopyroxene. Most grains are rounded or deeply etched. The etch pattern resembles that of clinopyroxene, but has an orthorhombic symmetry.

The distinctive pink-blue green pleochroism of orthopyroxene helps to identify this mineral, which never shows the nearly universal pale green color of clinopyroxene. However, much orthopyroxene is very pale in color. Site 292, Cores 1, 2, and 19 had some pale orthopyroxene, and Cores 3 through 7 and 17 had mostly the pale variety. At Site 296 pale orthopyroxene was found in Cores 1, 2, 5, 10, 16, 19, 22, 24, 27, and 28.

Zircon

Zircon was a scarce volcanic mineral, being principally associated with biotite. The biotite-rich ash from 296-28-4, 120 cm had crystals of zircon 10μ wide, but zircons in Samples 292-5-5, 24, 292-8-1, 127, and 296-15-2, 103 were much finer grained.

PATTERNS OF ERUPTIVE ACTIVITY

Table 1, and Figures 7 and 8, document the fact that the mineralogical character of ash depends somewhat on the amount of ash, i.e., the eruptivity shown by the sample. Thus, the relative amount of clear glass is highest in those samples which represent the largest eruptions. The more crystalline samples also occur during waning periods of eruption. Further, the relative amount of mafic minerals is lowest in the most abundant ash samples, and highest in samples with a limited ash content.

A further mineralogical distinction is worth noting. Orthopyroxene is a relatively abundant mafic mineral in ashes representing large eruptions (Figure 8), but hornblende is relatively more abundant during periods of limited activity (Figure 7). The two minerals show an antithetical relationship with eruptive activity, expressed as rate of accumulation of volcanic plagioclase.

The glass/crystal ratio and the orthopyroxene/hornblende ratio probably reflect the same phenomena. High eruptivity may result from bringing a very hot, almost completely liquid melt to the surface. A more crystallized melt has already lost much of its heat and, thus, potential explosive power. Because feldspars crystallize first and in the greatest abundance, and hornblende probably replaces orthopyroxene through magmatic reaction, the observed relationships are consistent with a model of variable extent of intratelluric crystalli-

zation. Further substantiation for the reaction of orthopyroxene in the melt is the observed rounding of grains completely invested with glass.

VOLCANIC HISTORY OF LUZON: SITE 292

The Tertiary tectonic evolution of Luzon is summarized by Gervasio (1973). Oligocene strata, aside from possible unfossiliferous early Oligocene beds, are absent, so historical inferences drawn from stratigraphy for this period are essentially impossible. This time period is represented by granitic stocks emplaced during an orogenic event. The early Miocene had "intermittent, but markedly reduced basaltic and andesitic effusions," followed by quartz diorite plutons in the middle Miocene. The late Miocene was a time of "thick and extensive dacitic tuffs and tuffaceous clastics, in places with associated andesitic and dacitic flows and agglomerates. . . The highly eruptive and siliceous volcanic activity extended to the early Pliocene." A later Plio-Pleistocene event formed "volcanic piedmont deposits around volcanic cones," and the extrusions of plateau basalts.

The present analysis (Figure 5) shows that the volcanic activity of Luzon in the Oligocene was moderate, rising to a maximum at the Oligocene-Miocene boundary. It fell off in the early Miocene, with the accumulation rate decreasing, and the number of samples with minimal ("trace") amounts of volcanic material increasing.

A hiatus recorded at Site 292 is followed by middle Miocene sediments showing moderate activity. This activity diminishes, but increases to another poorly defined maximum in the late Miocene (12 to 7 m.y.), with sporadic eruptions. At about 5 m.y. the activity increases, reaching a maximum during the Recent which is

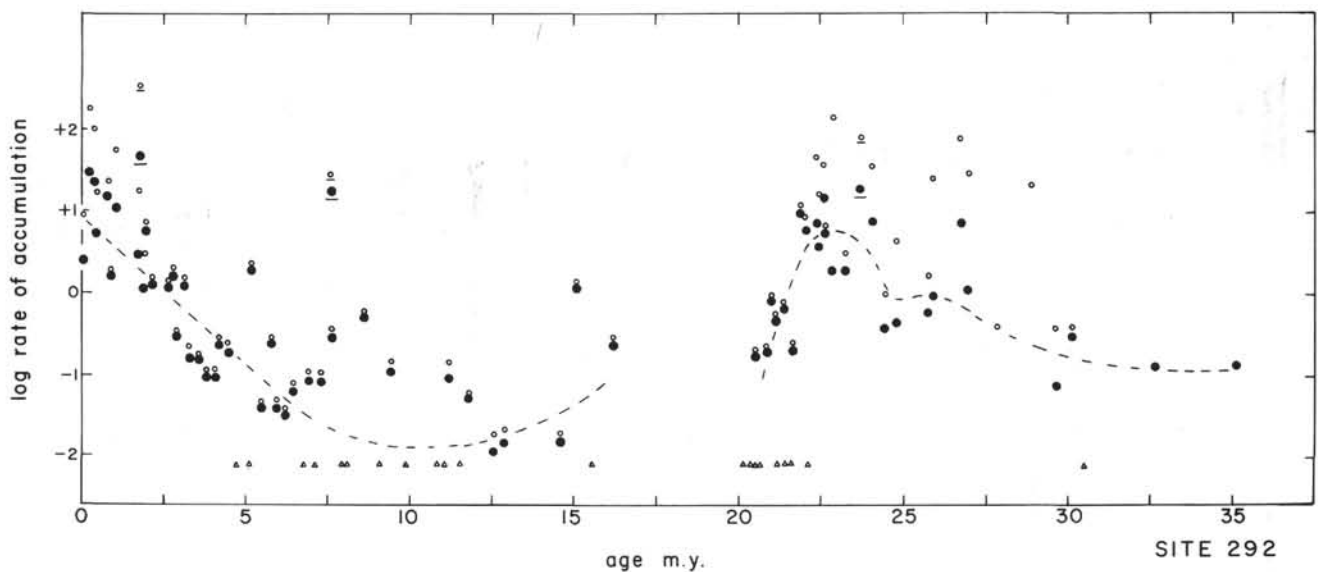


Figure 7. Plot showing for Site 292 the log of the accumulation rate for total volcanic debris (open circles) and plagioclase (solid circles) (g/cm^2 m.y.), against age of sediment. Dashed line shows trend for plagioclase. Tri-angles indicate samples with unmeasurably small quantities of volcanic debris. Underlined symbols are for samples labeled "ash."

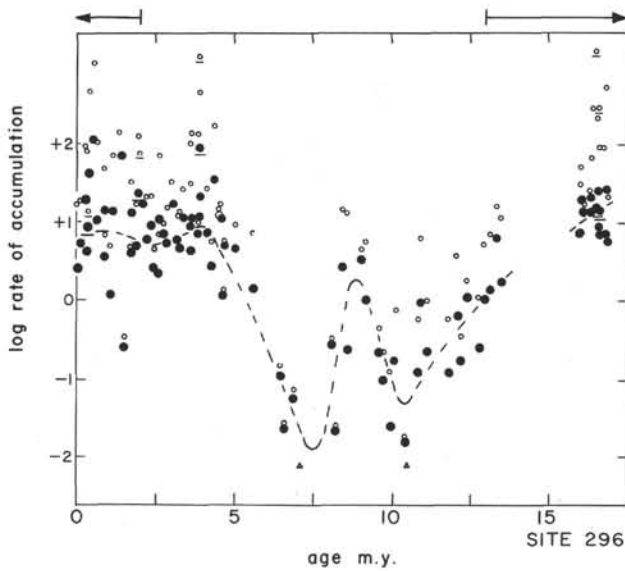


Figure 8. Plot showing for Site 296 the relationship between log accumulation rate versus age of sediment, as in Figure 7. Arrows at top show times of Neogene volcanic activity in central Japan (Sugimuro, personal communication).

quantitatively and qualitatively similar to that of about 22 m.y. ago.

The occurrence of quartz and epidote in the 22 m.y. to about 1.5 m.y. interval implies the transport of metamorphic debris from Luzon during that time by turbidity currents. The present bathymetry implies that such debris must have been carried a considerable distance uphill. This is a formidable difficulty not diminished by the inference that the paleobathymetry was similar.

In the Caribbean, turbidites from South America were traced to Sites 150 and 31 of DSDP Legs 15 and 4, respectively (Donnelly, 1973); again paleobathymetry would appear to require uphill transport, possibly as much as 1000 meters in the case of Site 31. The mechanism is not clear. Internal derivation of the debris from the crust of the Benham Rise is possible; the mineral assemblage is not definitive for either continental or oceanic crustal origin, although it does imply a low grade of metamorphism. Derivation of the debris from Luzon, however, requires that this derivation cease in the Pleistocene with the growth of the Philippine Trench and its northward extension, which became an efficient sediment trap for debris from Luzon.

VOLCANIC HISTORY OF SOUTHERN JAPAN: SITE 296

Debris on the Palau-Kyushu Ridge is presumed to come principally from southwestern Japan (Kyushu, southwestern Honshu) and the Ryukyu Islands; some component may be derived from the central Japan-Izu Islands volcanic trend (Figure 1). This latter derivation would require transport of coarse debris in a southward or westward direction, in opposition to the eastward-moving high-altitude winds. There seems to be no adequate mineralogical criterion for a separation of two

source belts, and there is no hint in the present work that multiple volcanic provenance areas may be involved.

Sugimura and Uyeda (1973) discuss the geologic development of western Japan primarily by analogy with better-known east Japan provinces. In southwestern Japan, volcanic activity was considered to be more important in the pre-Neogene, although some spectacular volcanic centers, such as Aso, remain to the Recent. Sugimura and Uyeda note that tholeiitic magmatic activity of the "northern zone" (Sea of Japan side of southwestern Honshu) of the early Miocene gave way to subalkalic activity in the middle and late Miocene of the median zone (of southwestern Honshu). From a variety of evidence they conclude, "...the sinking rate of the ocean lithosphere underthrusting the southwest Honshu Arc decreased from the early Miocene to the middle Miocene. A maximum in the middle Miocene was followed by the peak of activity in the late Miocene. The whole activity seems to have ended in the early Pleistocene Epoch."

In eastern Japan, Sugimura and Uyeda conclude that the volume of early Neogene (about 25 to 22 m.y.) volcanic material was about 50,000 km³/m.y., about 1000 km³/m.y. during the mid-late Neogene (22 to 2 m.y.), increasing to 2500 km³/m.y. in the last 2 m.y. Sugimura (personal communication) has recently extended the younger boundary of the early Neogene to 13 m.y.

The present study (Figure 6) largely confirms the two-stage (early Neogene and Quaternary) groupings of Sugimura and Uyeda, but adds some important information. The early Neogene volcanic activity declined to a minimum value in the middle Miocene (about 11 m.y.), and increased sharply to a short-lived peak about 9 m.y. It declined again in the late Miocene and increased sharply at the Miocene-Pliocene boundary. The late period of intense activity from 5 m.y. to the present might be divisible into an early and late more active period and a middle, less volcanic, period.

CONCLUSIONS

The deep-sea volcanic ash study presented here substantiates the previous work of Sugimura and Uyeda (1973), but refines their results. The striking rise of volcanic activity at 5 m.y. correlates at Sites 292 and 296, though the rise is far more dramatic at Site 296. Unpublished data from Central America (DSDP Site 83) and the results from the Lesser Antilles (Donnelly, 1973) further suggest a very widespread, perhaps worldwide, change in volcanic activity of subduction zones. The implied change in spreading rates of the world ocean is not as apparent. However, a recent study in the northeast Pacific (Blakley, 1974) shows that for the 17 m.y. to 9 m.y. period, the inferred spreading rate decreased gradually by about one-half to about 10 m.y. and rose abruptly to the earlier high value at 9 m.y. It may be coincidental that the volcanic activity curve for Site 296 is precisely parallel to this, but Site 292 shows only a poor parallel trend.

The results presented herein appear to provide an insight into a new question of global tectonics: is sea-floor spreading directly related to calcalkaline volcanic activity, does it vary with time, and on a worldwide basis?

ACKNOWLEDGMENTS

Sample preparation work for the present study was financed by a grant from the University Awards Committee of the State University of New York, and by further help from the Center for Solid Earth Geology of the State University of New York at Binghamton. Able assistance was provided by Bruce Gaither, Mark Griswold, and Roy Wilkens, to whom I am very grateful.

I am further grateful to Arata Sugimura for numerous stimulating discussions on the subject of Japanese volcanic history during his visit to this department, as well as for more recent correspondence on the subject.

REFERENCES

- Blakley, R.J., 1974. Fine-scale variation in spreading rates in the northeast Pacific (abstract): *EOS Am. Geophys. Union Trans.*, v. 55, p. 299.
- Donnelly, T.W., 1973. Circum-Caribbean explosive volcanic activity: evidence from Leg 15 sediments. *In* Edgar, N.T., Saunders, J.B., et al., Initial Reports of the Deep Sea Drilling Project, Volume 15: Washington (U.S. Government Printing Office), p. 966-988.
- Donnelly, T.W. and Nalli, G., 1973. Mineralogy and chemistry of Caribbean sediments. *In* Edgar, N.T., Saunders, J.B., et al., Initial Reports of the Deep Sea Drilling Project, Volume 15: Washington (U.S. Government Printing Office), p. 929-962.
- Gervasio, F.C. 1973. Geotectonic development of the Philippines. *In* Coleman, P.J. (Ed.), The Western Pacific: Island Arcs, Marginal seas. *Geochemistry*: (Univ. of Western Australia Press), p. 307-324.
- Kuno, H., 1962. Catalogue of the active volcanoes and solfatara fields of Japan, Taiwan, and Marianas: Internat. Volcanological Assoc. (Catalogue of the Active Volcanoes of the World), Part 11, 332 p.
- Neumann van Padang, M., 1953. Catalogue of the active volcanoes and Solfatara fields of the Philippine Islands and Cochin China: Internat. Volcanological Assoc. (Catalogue of the Active Volcanoes of the World), Part 2, 49 p.
- Sugimura, A. and Uyeda, S., 1973. Island Arcs: Japan and its environs: New York (Elsevier).

PLATE 1

Typical glass textures (scale bar is 100 μ m long)

- | | |
|----------|---|
| Figure 1 | Bubble glass; late Oligocene; 292-22-2, 57 cm. |
| Figure 2 | Tubular pumice; platy glass; Pleistocene; 296-2-6, 65 cm. |
| Figure 3 | Platy glass; large hornblende crystal; Pleistocene; 296-3-2, 131 cm. |
| Figure 4 | Platy glass; etched clinopyroxene crystal; Pliocene; 296-12-1, 98 cm. |
| Figure 5 | Tubular pumice; bubble glass, showing color variation; middle Miocene; 296-28-3, 96 cm. |
| Figure 6 | Bubble glass, biotite crystal; middle Miocene; 296-28-4, 120 cm. |

PLATE 1

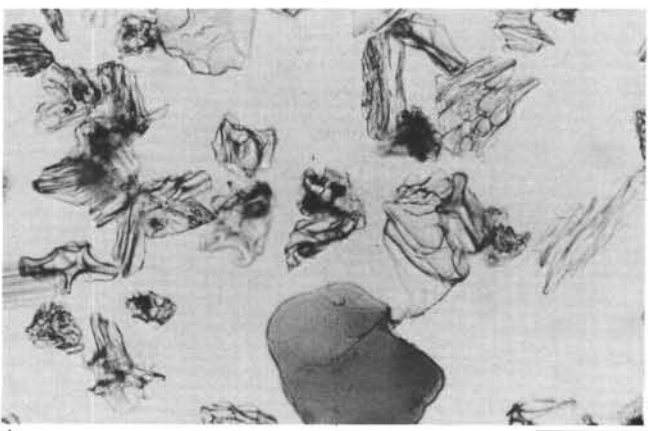
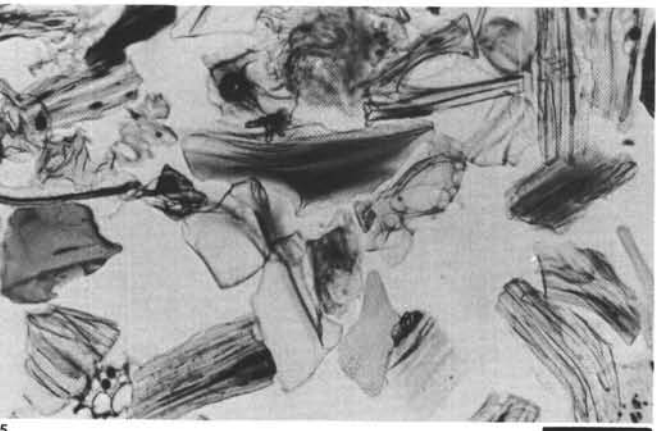
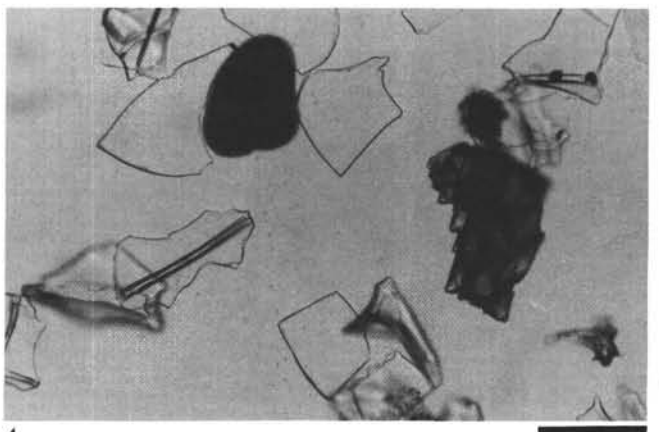
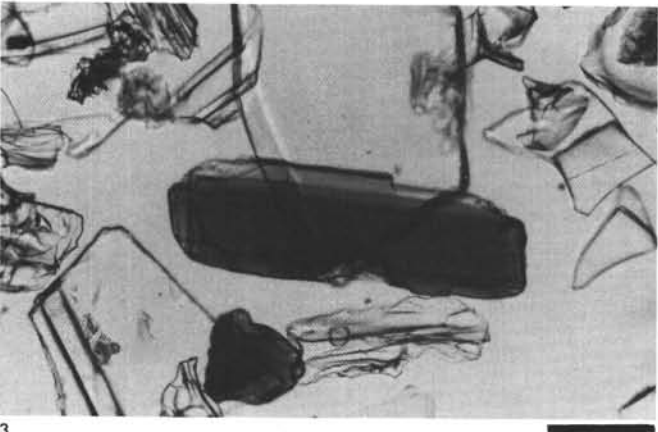
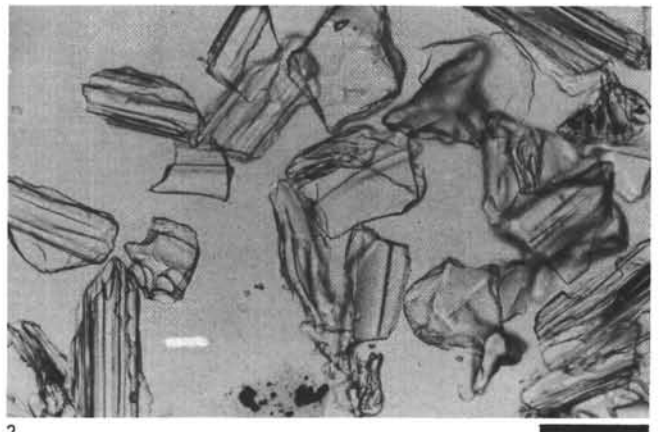


PLATE 2

Volcanic crystals and glass textures (scale bar is 100 μ m long)

- Figure 1 Magmatically rounded hornblende crystal invested with glass; bubble glass; Pleistocene; 292-1-4, 7 cm.
- Figure 2 Degraded glass remnant; Pleistocene; 292-2-2, 66 cm.
- Figure 3 Hornblende crystals, showing range in colors from pale to highly absorbent; Pliocene; 292-4-1, 91 cm.
- Figure 4 Degraded glass remnant (center); plagioclase; hornblende; late Miocene; 292-5-6, 60 cm.
- Figure 5 Biotite crystal (top center); etched clinopyroxene crystal (top right); plagioclase crystal (right center); middle Miocene; 292-8-3, 77 cm.
- Figure 6 Unetched orthopyroxene crystal; bubble glass; Pleistocene; 296-1-3, 77 cm.
- Figure 7 Porphyritic glass; middle Miocene; 296-22-1, 141 cm.
- Figure 8 Bubble glass, showing color variation; early Miocene; 296-28-2, 84 cm.

PLATE 2

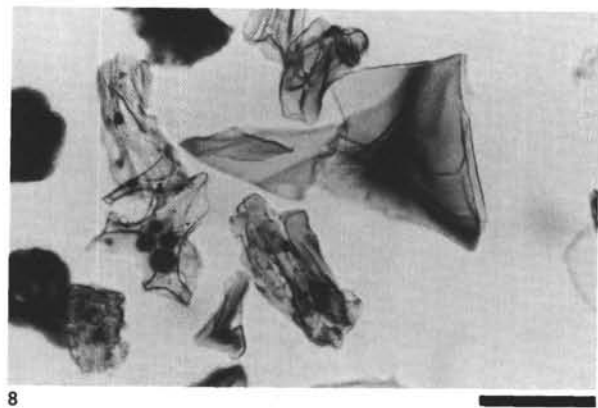
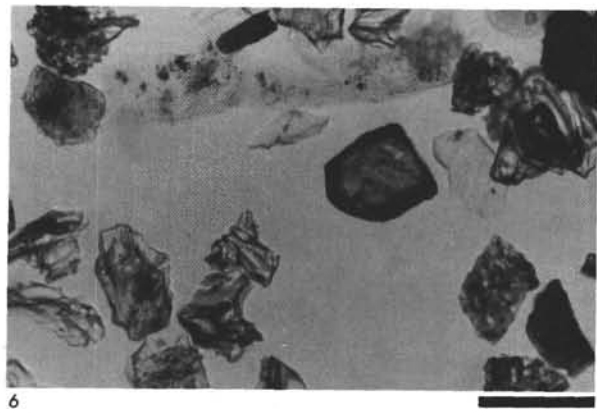
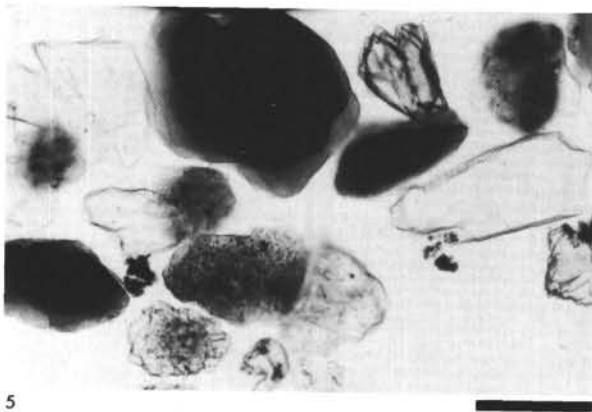
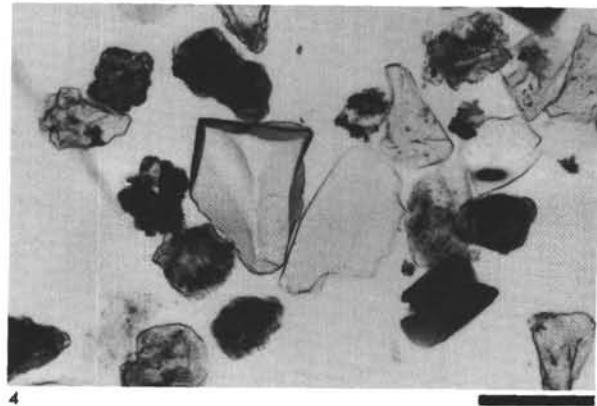
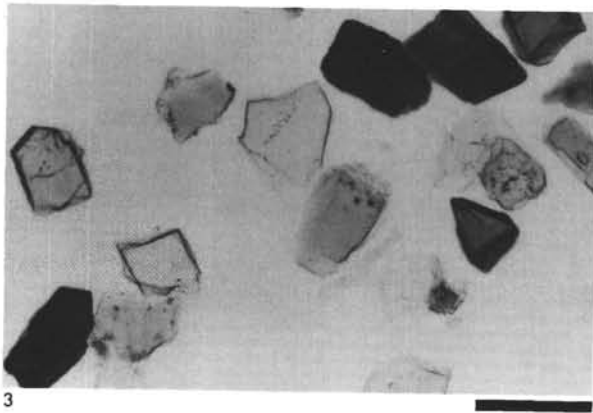
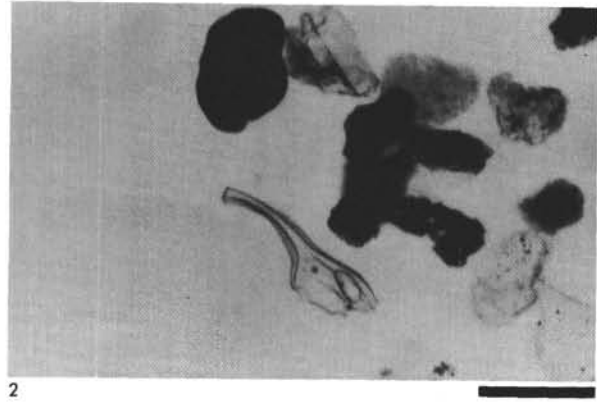
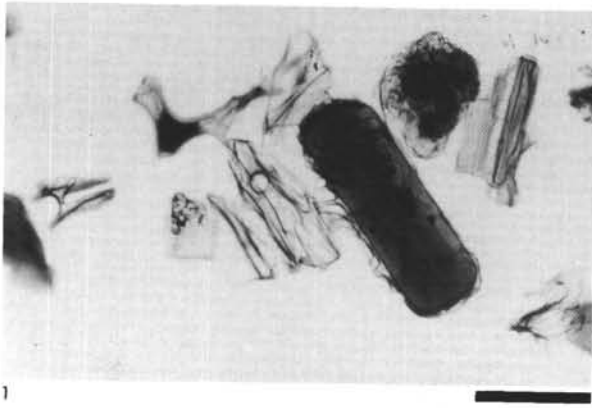


PLATE 3

Authigenic minerals; volcanic crystals (scale bar is 100 μ m long)

- Figure 1 Magmatically rounded clinopyroxene invested with glass (right center); brown (basaltic) glass (left center); Pleistocene; 292-1-1, 74 cm.
- Figure 2 Riebeckite euhedron; glass fragments; late Eocene; 292-36-1, 18 cm.
- Figure 3 Authigenic glaucophane crystal (center); late Eocene; 292-36-1, 18 cm.
- Figure 4 Unetched clinopyroxene euhedron; glass fragments; late Eocene; 292-36-1, 18 cm.
- Figure 5 Authigenic K-feldspar crystal; late Pliocene; 296-11-4, 33 cm.
- Figure 6 Authigenic K-feldspar euhedron; early Miocene; 296-26-5, 102 cm.

PLATE 3

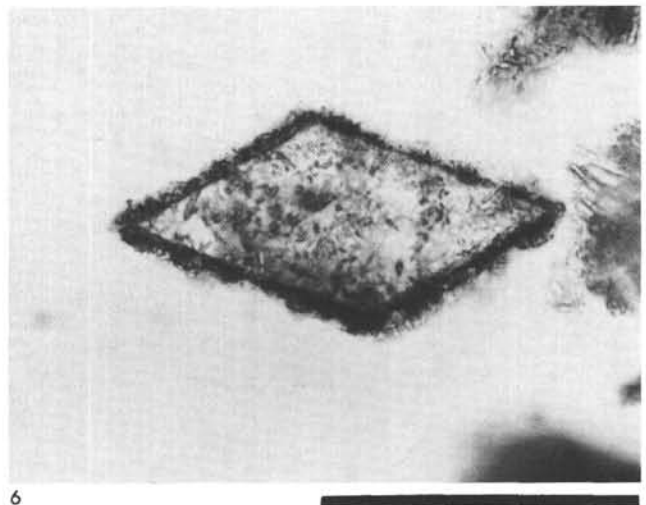
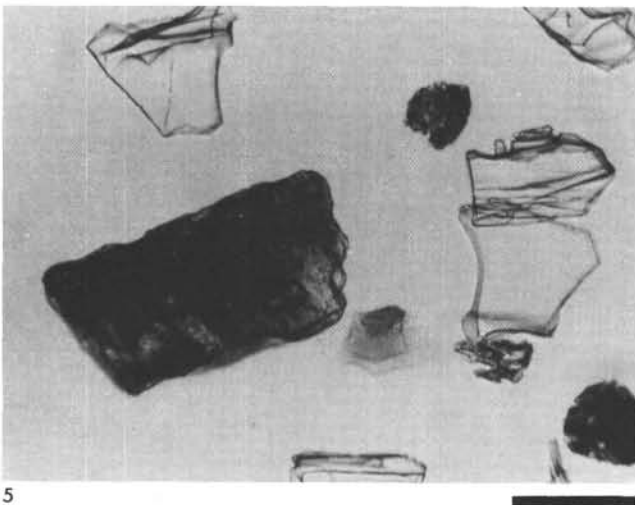
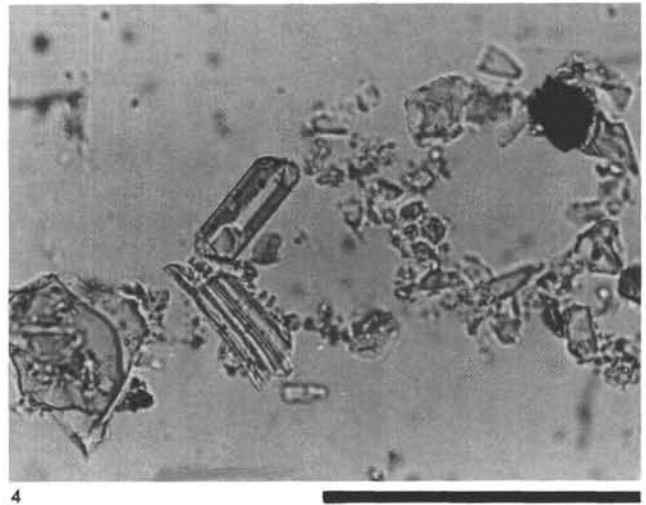
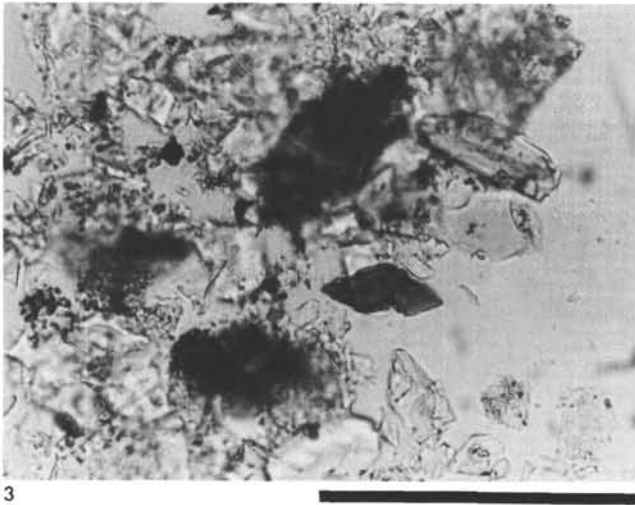
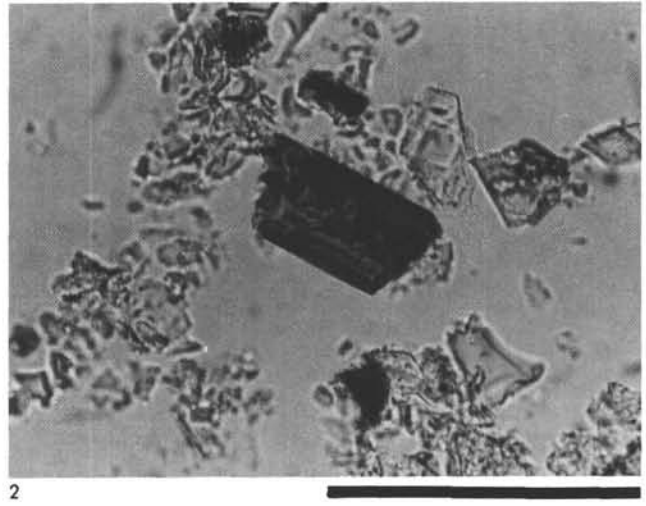
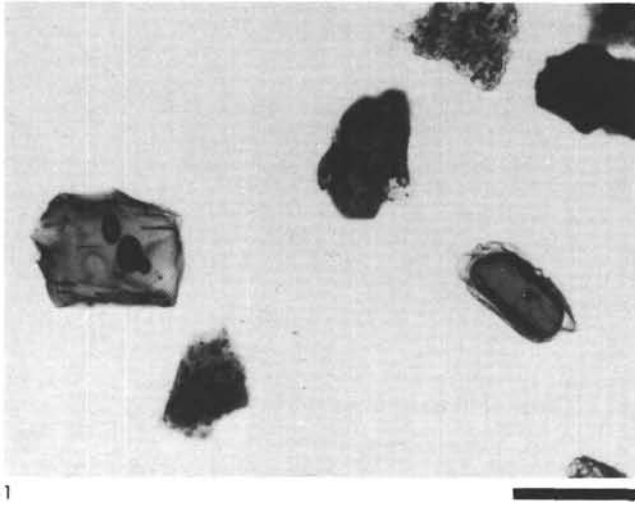
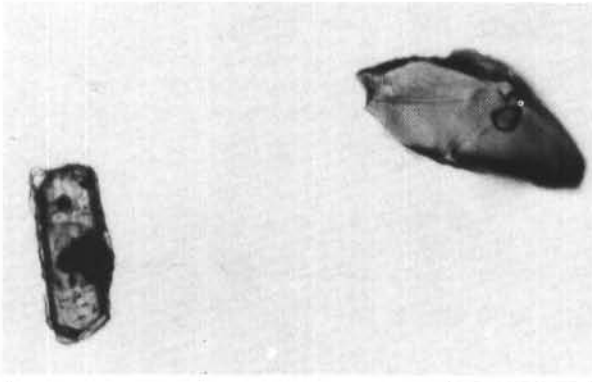


PLATE 4

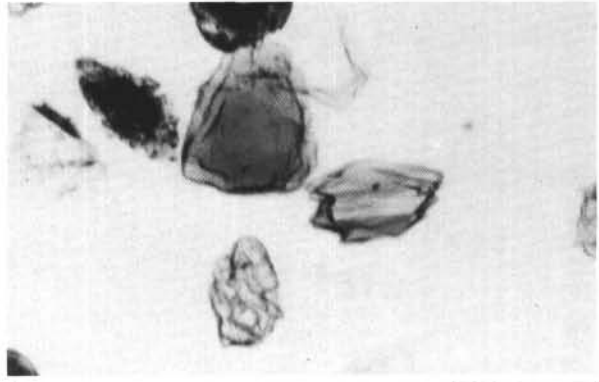
Volcanic crystals; zeolite: glass (scale bar is 100 μ m long)

- Figure 1 Fractured (right) and euhedral, glass invested clinopyroxene (left) crystals; Pleistocene; 292-1-1, 74 cm.
- Figure 2 Etched clinopyroxene; hornblende crystals; late Pliocene; 292-3-4, 30 cm.
- Figure 3 Etched orthopyroxene; late Oligocene; 296-21-5, 133 cm.
- Figure 4 Etched clinopyroxene; late Oligocene; 296-21-5, 133 cm.
- Figure 5 Etched orthopyroxene; late Pliocene; 296-11-4, 33 cm.
- Figure 6 Brown (basaltic) glass and clear glass, showing relief contrast; Pleistocene; 296-5-1, 115 cm.
- Figure 7 Zeolite "lump" (center, highest relief); clinopyroxene fragment (right center); glass fragments; late Pliocene; 296-8-3, 123 cm.
- Figure 8 Zeolite "lump" (right, highest relief); clinopyroxene (left center); plagioclase; early Miocene; 296-27-2, 124 cm.

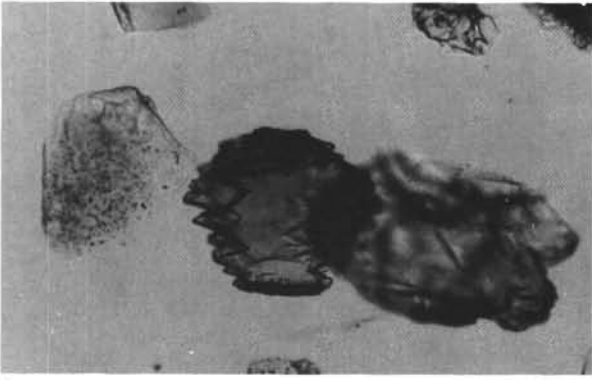
PLATE 4



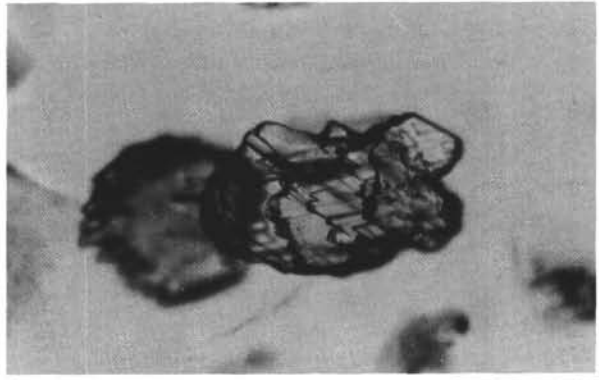
1



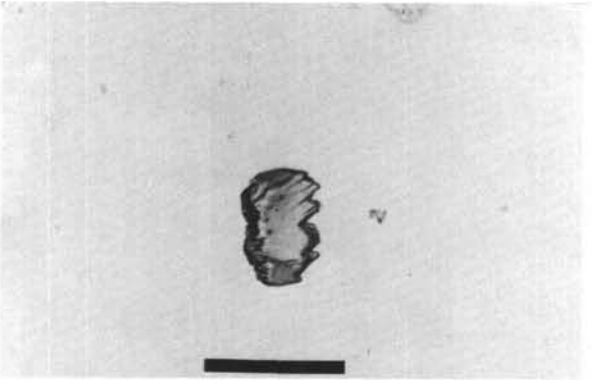
2



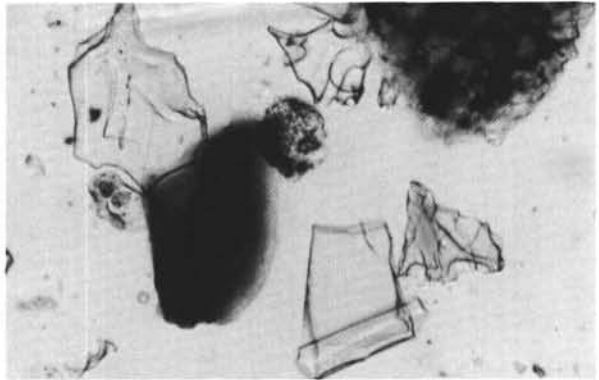
3



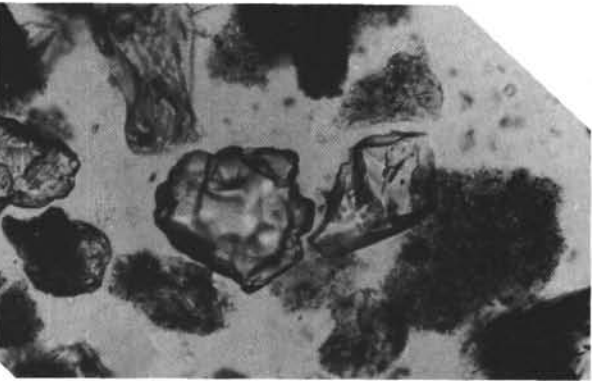
4



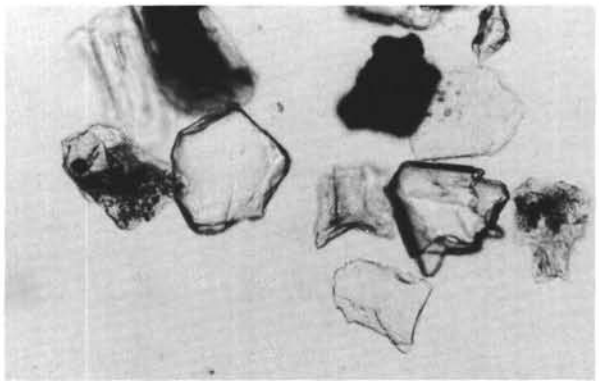
5



6



7



8